Acta Oceanol. Sin., 2018, Vol. 37, No. 1, P. 1–10
DOI: 10.1007/s13131-018-1153-0
http://www.hyxb.org.cn
E-mail: hyxbe@263.net

Parameterizing sea surface temperature cooling induced by tropical cyclones using a multivariate linear regression model

WEI Jun[1]*, LIU Xin[2, 1], JIANG Guoqing[1]

[1] Laboratory for Climate and Ocean-Atmosphere Studies, Department of Atmospheric and Oceanic Sciences, Peking University, Beijing 100871, China

[2] State Key Laboratory of Severe Weather, Chinese Academy of Meteorological Sciences, Beijing 100081, China

Received 23 January 2017; accepted 20 June 2017

Abstract

Combining a linear regression and a temperature budget formula, a multivariate regression model is proposed to parameterize and estimate sea surface temperature (SST) cooling induced by tropical cyclones (TCs). Three major dynamic and thermodynamic processes governing the TC-induced SST cooling (SSTC), vertical mixing, upwelling and heat flux, are parameterized empirically using a combination of multiple atmospheric and oceanic variables: sea surface height (SSH), wind speed, wind curl, TC translation speed and surface net heat flux. The regression model fits reasonably well with 10-year statistical observations/reanalysis data obtained from 100 selected TCs in the northwestern Pacific during 2001–2010, with an averaged fitting error of 0.07 and a mean absolute error of 0.72°C between diagnostic and observed SST cooling. The results reveal that the vertical mixing is overall the pre dominant process producing ocean SST cooling, accounting for 55% of the total cooling. The upwelling accounts for 18% of the total cooling and its maximum occurs near the TC center, associated with TC-induced Ekman pumping. The surface heat flux accounts for 26% of the total cooling, and its contribution increases towards the tropics and the continental shelf. The ocean thermal structures, represented by the SSH in the regression model, plays an important role in modulating the SST cooling pattern. The concept of the regression model can be applicable in TC weather prediction models to improve SST parameterization schemes.

Key words: tropical cyclones, SST cooling, regression model, parameterization

Citation: Wei Jun, Liu Xin, Jiang Guoqing. 2018. Parameterizing sea surface temperature cooling induced by tropical cyclones using a multivariate linear regression model. Acta Oceanologica Sinica, 37(1): 1–10, doi: 10.1007/s13131-018-1153-0

1 Introduction

Sea surface temperature (SST) cooling can be induced by tropical cyclones (TCs) in the upper ocean. They are often observed from satellite images on both sides of a TC's track, with maximum SST cooling along its right hand side. The rightward bias of the SST cooling can be attributed to TC wind stress vectors turning clockwise in time on the right side of the track which is roughly resonant with TC-induced near-inertial rotating currents (Price, 1981; Shay et al., 1992; Price et al., 1994; Cione and Uhlhorn, 2003). The TC-induced SST cooling (hereafter SSTC) is mainly controlled by two oceanic internal processes, vertical mixing and upwelling, and by surface heat flux under TC conditions. The vertical mixing in the upper ocean induced by TC wind stress is associated with an entrainment process, which mixes surface warm water and deep cold water and consequently deepens the ocean mixed layer. The entrainment rate is proportional to the wind stress acting on the ocean surface (Price, 1981; Ginis, 2002). The upwelling can be produced by Ekman pumping and near-inertial oscillations of ocean currents (Price et al., 1994; Shay et al., 2000; Jaimes and Shay, 2009). The Ekman-induced upwelling occurs throughout the entire water column underneath the TC center, mainly driven by cyclonic TC wind curl (Liu and Wei, 2015). The upwelling associated with the near-inertial current oscillations is due to surface flow divergence. On the other hand, strong typhoon winds can enhance local evaporation, leading to more latent heat loss from the ocean, and thus a cooling down of the ocean surface. Some previous studies reveal that the heat flux forcing can contribute significantly to the total SSTC (Jacob et al., 2000; Huang et al., 2009; Vincent et al., 2012). However, this cooling will be mixed immediately by wind-induced vertical mixing, and therefore is rather difficult to isolate the heat flux effect from those of ocean internal processes.

The relative roles of the dynamic and thermodynamic processes underlying the SSTC had been extensively investigated in previous studies. Jullien et al. (2012) found that vertical mixing can largely explain the SSTC during a TC's passage, while SST cooling associated with baroclinic near-inertial ocean oscillations is insignificant. In contrast, upwelling associated with barotropic Ekman pumping plays an important role on the subsurface that can last for a longer time period than surface cooling. On a mixed layer ocean model with idealized TC experiments, Price (1981) also found that the vertical mixing dominates in the

Foundation item: The Major National Basic Research Development Program of China under contract No. 2016YFA0202704; the National Natural Science Foundation of China under contract Nos 41476008 and 41576018; the Basic Fund of Chinese Academy of Meteorological Sciences under contract No. 2017Z017; the Strategic Priority Research Program of the Chinese Academy of Sciences under contract No. XDA11010303.
*Corresponding author, E-mail: junwei@pku.edu.cn

total SSTC (>85%), while both upwelling and heat flux forcing account for less than 15%. This model result was supported later by observations in Jacob et al. (2000). On a three-dimensional primitive equation ocean model, we obtained a similar result in a case study of Typhoon Megi (2004) (Wei et al., 2014). The vertical mixing-induced ocean temperature cooling accounts for 75% of the total SSTC in the open ocean and can be up to 99% in the Kuroshio and over the continental shelf, while the upwelling-induced cooling is prominent only on the subsurface, especially after Typhoon Megi's passage. Furthermore, SSTC is sensitive to TC translation speeds. Bender and Ginis (2000) grouped the SSTC according to the slow, medium and fast moving TCs, resulting in average cooling for the three groups of 5.3, 3.5 and 1.8°C, respectively. Price (1981) showed that the upwelling-induced cooling became significantly important for slow-moving TCs. The rightward bias of the SST cooling becomes prominent when the TC translation speed is equivalent to the local inertial frequency.

On the other hand, the SSTC depends on subsurface ocean conditions as well. Wu et al. (2008) found significant SST cooling over the continental shelf of the East China Sea during Typhoon Nari's (2001) passage and attributed it to shallow thermocline. Sakaida et al. (1998) found 9°C cooling in the Kuroshio Extension area due to a sharp temperature gradient below the sea surface. Wei et al. (2014) found that strong temperature cooling within the Kuroshio during the TC's passage was related to pre-existing strong baroclinic currents that significantly enhance local vertical mixing. In contrast, based on a case study of Super-typhoon Maemi (2003) and 30 category-5 typhoons, Lin et al. (2005, 2008) claimed that warm ocean features with a deep thermocline, such as warm eddies, could significantly restrain the SSTC and therefore favor TC rapid intensification. Sun et al. (2015) found that the SST cooling induced by Typhoon Nuri (2008) is increased when Nuri propagated from western Pacific towards the South China Sea, due to shoaling of the mixed layer depth between the two ocean basins.

As revealed by previous studies, the SSTC is a very complex process, involving combinations of dynamic and thermodynamic processes under different TC and oceanic conditions. To account for the SSTC effect, a time-dependent SST is the most common way for TC weather prediction models to specify their ocean surface conditions, for example, using daily updated satellite SST data (Chelton, 2005; Zhu and Zhang, 2006; Vincent et al., 2012). However, the presence of precipitating clouds prevents the instantaneous satellite detection of the TC-induced cooling, so the operational satellite data may contain a time lag in the SST cooling feedback and thus warm bias for the atmospheric models (Braun, 2002; Chen et al., 2011). Furthermore, the spatial and temporal resolutions of the satellite-detected SST cooling are very coarse for some TC modeling studies. On the other hand, although the coupled air-sea models have many obvious advantages for modeling the SSTC, their practical applications may prove to be challenging. For example, the lack of high-resolution observations over vast oceans makes it hard to provide a realistic initial field for ocean models. Therefore, how to estimate the TC-SSTC condition using a simple, fast, robust and effective SST parameterization becomes highly desirable for a TC-ocean research community.

In this study, a multivariate regression model was proposed to parameterize the dynamic and thermodynamic processes underlying the SSTC, which can provide a flow-dependent SST condition for TC forecast models. The next section describes the data source and methodology used for this study. In Section 3, 10-year statistical observations/reanalysis data during periods of 100 selected TCs in the northwestern Pacific from 2001 to 2010 were used to verify the effectiveness of the regression model. The regression results in turn were used to further understand the mechanisms of the TC-SSTC from a statistical point of view. A summary and concluding remarks are given in Section 4.

2 Data source and methodology

2.1 *Data source*

The data used in this study can be categorized into atmospheric variables (winds and net heat flux) and oceanic variables (SST, SSH and ocean depth). Surface winds were obtained from a 6-h cross-calibrated multi-platform (CCMP) product with a resolution of 0.25°×0.25° (http://rda.ucar.edu/datasets/ds744.9/). The winds are used to represent the strength of the ocean mixing. Although we note that the CCMP winds are generally underestimated compared with actual TC intensities, the regression model relies only on the variability of the CCMP winds, instead of its actual amplitudes, due to the normalization described in the data preprocessing. Surface net heat fluxes, consisting of latent heat, sensible heat, short-wave and long-wave radiative heat fluxes, were obtained from 6-h NCEP-DOE reanalysis 2 with a relatively coarser resolution of 2.5°×2.5° (http://www.esrl.noaa.gov/psd/data/gridded/data.ncep.reanalysis2). Given that, the surface heat fluxes usually contribute less than 20% of the total SSTC (Jacob et al., 2000; Vincent et al., 2012), and that, among the total heat fluxes, the large-scale wind-induced latent heat is dominated, the heat flux forcing is less important than other variables in resolving fine structures of the SSTC. To examine its relative importance, in the discussion section, we present and discuss the regression model with and without the heat flux forcing.

Satellite-derived SSTs were used in the regression model to determine the model coefficients. The SST maps were obtained from tropical rainfall measuring mission/microwave imager (TRMM/TMI) which provides cloud-penetrating daily SST with a resolution of 0.25°×0.25° from 1997 to the present (http://pmm.nasa.gov/TRMM). TMI SSTs have been widely used in the observational analysis of the SSTC. But they are rarely used for TC modeling studies, because of considerable amount of missing data. The SSH was acquired from archiving, validation, and interpretation of satellite oceanographic data (AVISO) (http://www.aviso.oceanobs.com) with a resolution of 0.25°×0.25°. The ocean depth was obtained from the ETOPO5 database with a resolution of (1/12)°×(1/12)°.

The above atmospheric and oceanic data were extracted from corresponding periods of selected TCs' life time. TC information was obtained from the best-track data supplied by the Joint Typhoon Warning Center (JTWC, http://www.usno.navy.mil/JTWC), which provides 6-h real time trajectories and intensities from 1948 to the present. According to the JTWC records, there were a total of 363 TCs in the northwestern Pacific during 2001–2010. In this study, 100 TCs were selected with maximum ocean surface cooling larger than 2°C. Figure 1 shows trajectories and intensities (maximal winds) of the 100 selected TCs. Note that the trajectory information is from the JTWC and the wind speeds are from CCMP dataset, because the latter is used in the regression model. We see that the 100 TC trajectories spread over the northwestern Pacific with about 90% of the TCs along the typical storm track and 10% propagated into the South China Sea.

2.2 *Regression model*

A regression model was proposed based on a primitive temperature budget equation, which can be written as follows:

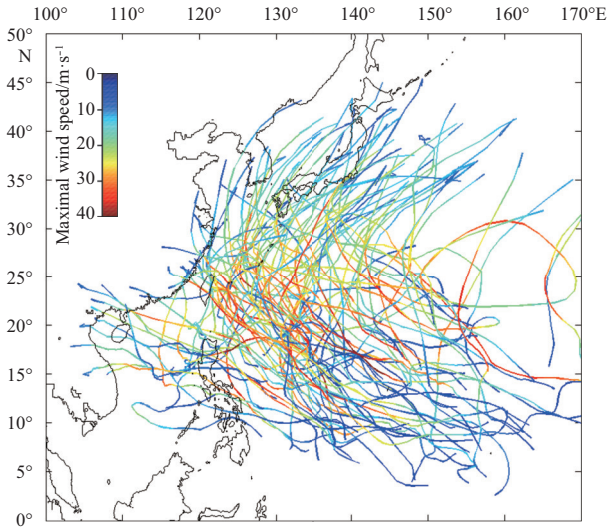

Fig. 1. Trajectories of 100 selected TCs colored by maximal wind speeds (m/s). The trajectory information is from JTWC. The maximal wind speeds are from CCMP dataset which is used in the regression model.

$$\underbrace{\frac{\partial T}{\partial t}}_{\mathrm{T}}=\underbrace{K\frac{\partial^2 T}{\partial Z^2}}_{\mathrm{MIX}}\underbrace{-\left(u\frac{\partial T}{\partial x}+v\frac{\partial T}{\partial y}+w\frac{\partial T}{\partial z}\right)}_{\mathrm{ADV}}+\underbrace{\frac{\partial}{\partial x}\left(A_{\mathrm{h}}\frac{\partial T}{\partial x}\right)+\frac{\partial}{\partial y}\left(A_{\mathrm{h}}\frac{\partial T}{\partial y}\right)}_{\mathrm{HDIF}}+\underbrace{\frac{Q}{h\rho_0 C_p}}_{\mathrm{HFX}}. \quad (1)$$

The left-hand side term is the rate of temperature change; u, v and w are the ocean current velocities in the x, y and z directions, respectively; A_{h} and K are horizontal and vertical diffusivity; C_p is the specific heat of water; ρ_0 is the water density; and h is the mixed layer depth. The right-hand side terms represent vertical mixing (MIX), advection (ADV), horizontal diffusion (HDIF), and heat flux forcing (HFX), respectively. The horizontal diffusion term can be neglected under TC conditions since it had been shown to be very small compared with the other terms (Price, 1981; Uhlhorn and Shay, 2013; Wei et al., 2014). Thus, Eq. (1) can be simplified as follows:

$$\underbrace{\frac{\partial T}{\partial t}}_{\mathrm{T}}=\underbrace{K\frac{\partial^2 T}{\partial Z^2}}_{\mathrm{MIX}}\underbrace{-V\cdot\nabla T}_{\mathrm{ADV}}+\underbrace{\frac{Q}{h\rho_0 C_p}}_{\mathrm{HFX}}, \quad (2)$$

where K is the vertical diffusivity (assuming to be a constant), and $K\frac{\partial}{\partial Z}$ represents the strength of the vertical temperature gradient. Then, the regression model of SST changes related to the three budget terms can be expected as

$$\triangle\mathrm{SST}=a\times\mathrm{MIX}+b\times\mathrm{ADV}+c\times\mathrm{HFX}, \quad (3)$$

where a, b and c are unknown coefficients reflecting relative weights for the individual term. ΔSST is defined as a SST difference relative to its initial value, that is, $\Delta\mathrm{SST}=\mathrm{SST}_0-\mathrm{SST}$ and SST_0 is the initial SST state. We noted that the right hand side terms represent a combined nonlinear effect of the three processes. To explicitly diagnose their relative contributions, a linear assumption was made, so that the coefficients a, b and c can be determined using least square fitting.

2.3 *Pre-processing of data*

To validate the effectiveness of the regression model, the model was fitted individually to the 100 selected TCs. The atmospheric and oceanic data applied to the regression model were screened according to the life period of each TC. First, for each grid point we defined a TC passage period from t_0 to t_1, where t_0 and t_1 are the time when the TC center is located at 450 km before and after the grid point. A constant of 450 km is chosen, given the common sizes of 400–500 km for typhoons (Lin et al., 2015). Second, the observed SST changes at each grid point used the maximum TMI SST difference during the TC period ($\mathrm{SST}_{\max}-\mathrm{SST}_{\min}$). The corresponding wind speeds and wind curl used their maximum values, too. In contrast, the SSH, heat flux and TC translation speed used their averages as these variables did not change much during the TC period.

Since most of the satellite data were available at a spatial resolution of 0.25°×0.25°, except for the heat fluxes, for consistency all data were first interpolated to a spatial resolution of 0.25°×0.25°. Furthermore, all variables were interpolated/averaged to a uniform temporal scale of daily average. Prior to being used in the regression model, in order to unify different units, all variables were normalized to a range of [0.5, 1.5] with their means equal to 1. This also avoids a near-zero value in the denominator and thus makes the model more stable. By doing so, it can be expected that the variations of all variables are scaling to the same order when performing the least-square fitting. In other words, the regression model essentially examines the fitness between the variability of the SSTC and that of the three budget terms, rather than their actual amplitudes.

3 Parameterizing the SSTC using the regression model

3.1 *Significance analysis of the typhoon statistics*

In order to parameterize Eq. (2), we first attempt to determine those atmospheric and oceanic factors that have a statistically significant effect on the SSTC. Figure 2 compares the composite maps of the observed SST cooling and other atmospheric/oceanic variables for the 100 selected TCs. Here, the SSTC for each typhoon is defined as the SST difference relative to its pre storm condition. From a statistical point of view, strong SST cooling occurs north of 20°N along the typical storm track (Fig. 2a), which is generally consistent with the map of the wind speeds (Fig. 2c). Notable cooling is also found in coastal seas, where low SSH implies a shallow thermocline (Fig. 2b). The wind curl (net heat flux) generally shows a similar (opposite) pattern to the map of the wind speeds, indicating that strong wind speeds are often accompanied with strong wind curl (cyclonic) and the negative heat flux (ocean losing heat through evaporation). On the other hand, the SSTC map in general also corresponds to the typhoon translation speeds (SPD) and latitudes to some extent, with slow (fast) translation speeds corresponding to small (large) SSTC at the low (high) latitudes (Fig. 2f).

To determine the significance of these atmospheric/oceanic factors, we calculate correlation coefficients (r) between the SSTC and other variables for each typhoon case (Fig. 3). As expected, the SST cooling is most sensitive to the winds and the net heat flux, with an almost linearly positive correlation with the wind speed/wind curl (Figs 3a and b), and a negative correlation with the heat flux (Fig. 3d). The ocean mixed layer depth can be indirectly inferred from the SSH, with higher SSH implying a deeper

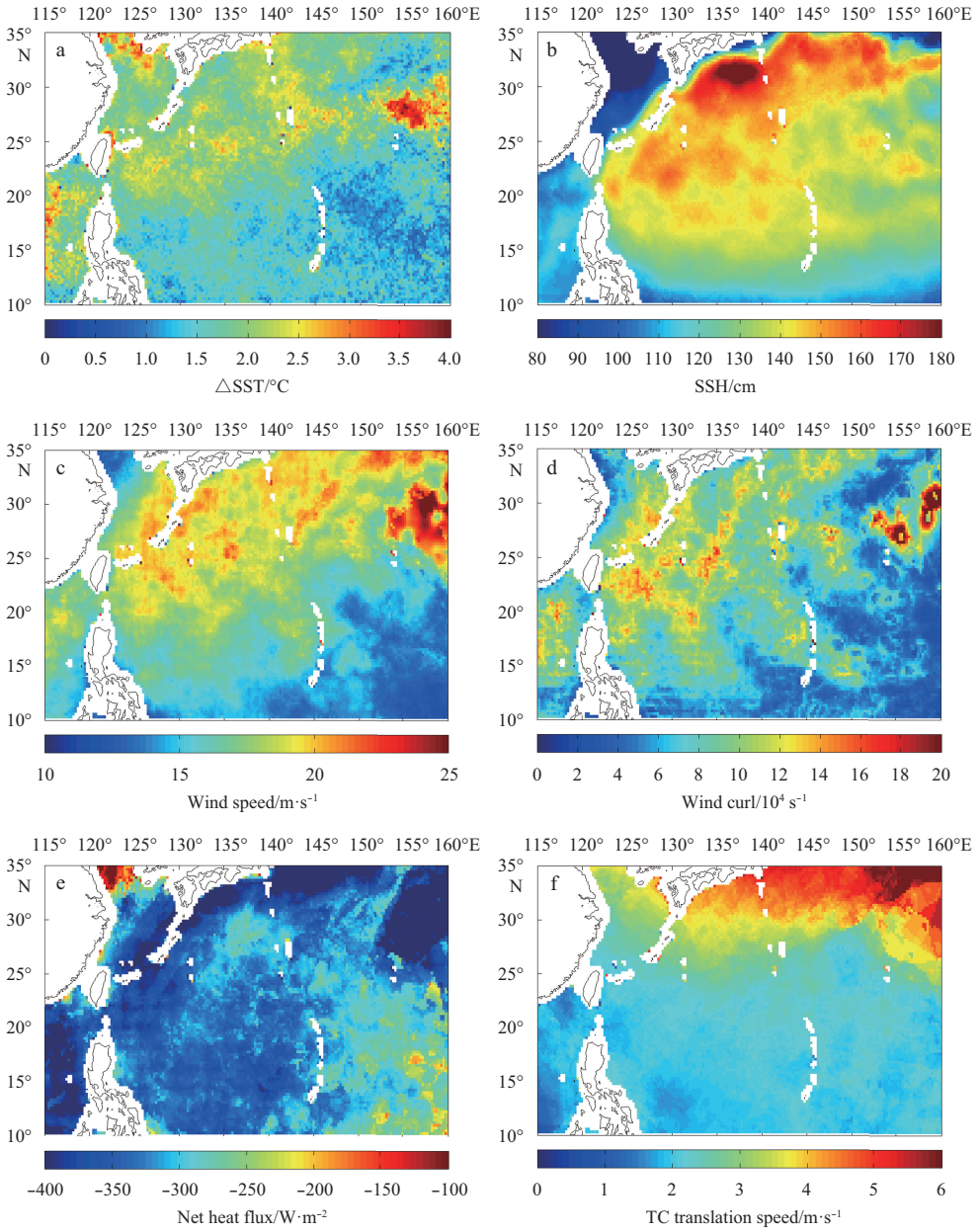

Fig. 2. Composite maps of ΔSST (°C, a), SSH (cm, b), wind speed (m/s, c), wind curl (10^4 s^{-1}, d), net heat flux (W/m^2, e) and TC translation speed (m/s, f). The maps are averaged over 100 selected TCs within 450 km radius along TC track.

mixed layer and vice versa. It can be seen that the SST cooling decreases with the SSH when the SSH is less than 100 cm (Fig. 3c), as a deeper mixed layer can restrain the entrainment process. The SST cooling slightly increases when the SSH is greater than 100 cm, which is likely influenced by winds. High SSH regions correspond to high-latitudes along the storm track (Fig. 2b) where the TCs are well developed (Fig. 2c). In contrast, the SST cooling is overall less sensitive to latitudes and the TC translation speeds (Figs 3e and f).

Figure 4 shows *r* between the observed SST cooling and other variables for individual TC. The results are basically consistent with Fig. 3. The SST cooling has the largest positive *r* with the wind speed/wind curl, and the negative *r* with the net heat flux. The SST cooling is shown statistically uncorrelated with the SSH and the TC translation speed due to their nonuniform correlations in different regions and scales (Figs 4c and d). Meanwhile, the combined effects of the atmospheric and oceanic variables on the total SST cooling are naturally interactive. For example, the wind effect apparently is the most dominant factor that can significantly influence the correlations of the SST cooling with other variables. To isolate its effects from other variables, we recalculated partial correlation coefficients (P- *r*) by controlling the wind-related variables (Fig. 5). It is shown that the SST cooling is now statistically uncorrelated with the net heat flux and latitude, as the net heat flux is highly correlated with winds and the increasing SST cooling with latitude is related to increasing TC intensity. On the other hand, the isolated effects of the SSH and the TC translation speed on the SST cooling become evident. Their negative P- *r* indicate that slow-moving TCs and small SSH favor large SST cooling which is consistent with the interpretations by Price (1981) and Wu et al. (2008).

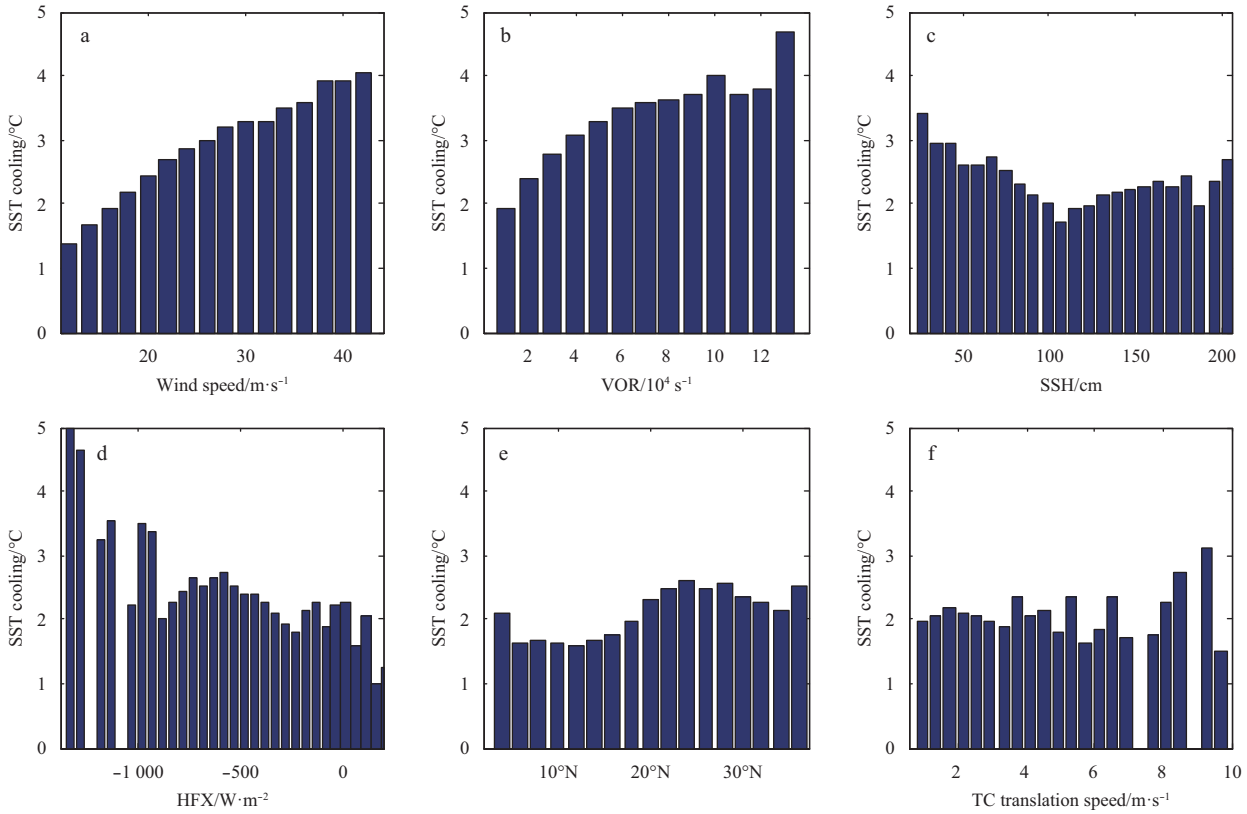

Fig. 3. Correlations between SST cooling and atmospheric/oceanic variables: a. wind speed, b. wind curl (vorticity), c. SSH, d. heat flux, e. latitude and f. TC translation speed.

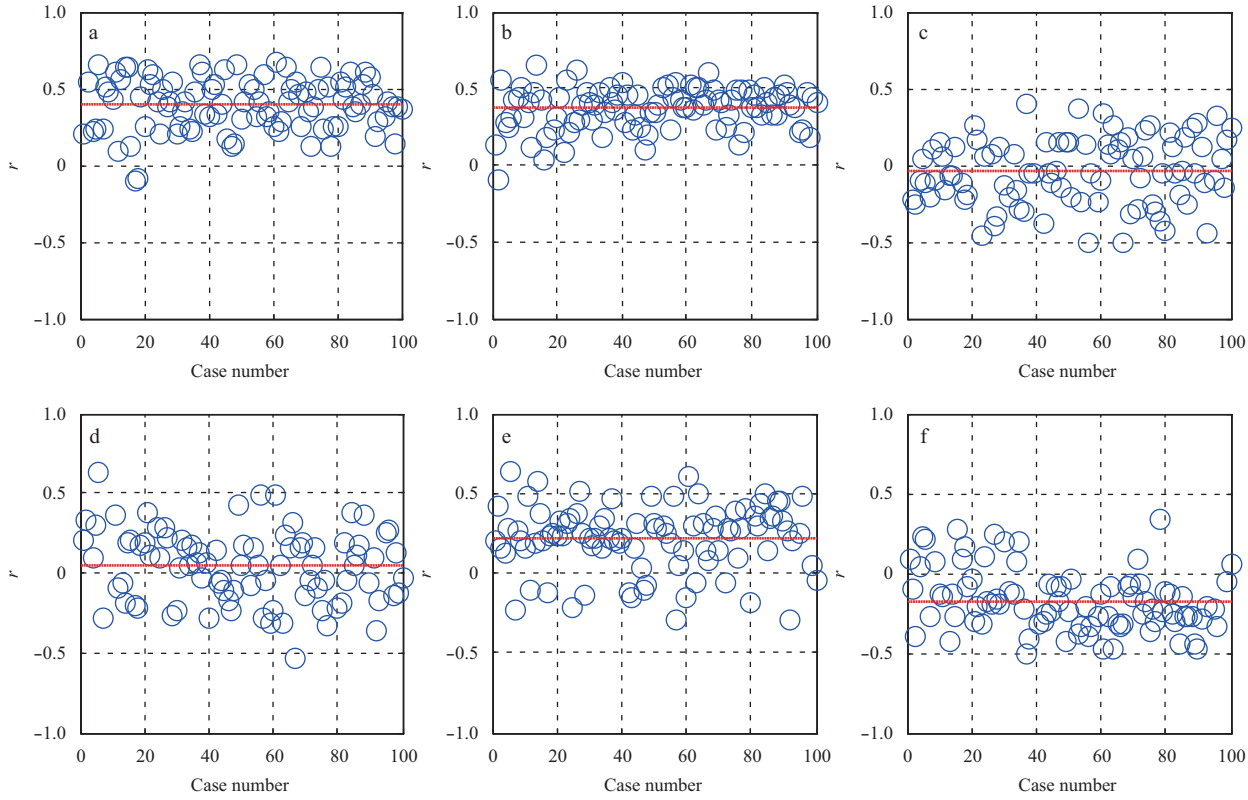

Fig. 4. Correlation coefficients between SST cooling and atmospheric/oceanic variables: a. wind speed, b. wind curl, c. SSH, d. TC translation speed, e. latitude and f. heat flux for 100 selected TCs. Correlation coefficients within 95% confidence interval are presented. Red lines indicate the mean values.

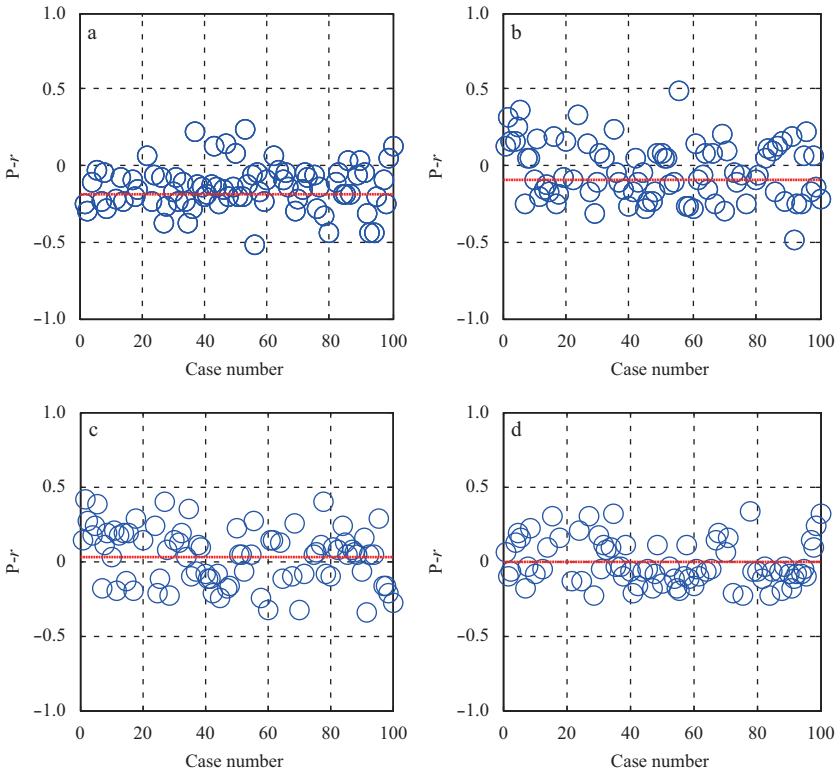

Fig. 5. Partial correlation coefficients between SST cooling and atmospheric/oceanic variables by controlling wind-related variables: a. SSH, b. TC translation speed, c. latitude and d. heat flux for 100 selected TCs. Correlation coefficients within 95% confidence interval are presented. Red lines indicate the mean values.

3.2 *Diagnostic SSTC with the regression model*

According to the sensitivity analysis, five variables (wind speed (*wnd*), wind curl (*curl*), net heat flux (*Q*), SSH, and TC translation speed (*SPD*)) were chosen for the regression model. Thus, the temperature Eq. (2) is further parameterized as follows:

$$\Delta SST_{diag} = a\times\frac{wnd}{SSH} + b\times\frac{curl(\tau)}{SPD} + c\times\frac{Q}{SSH} + \varepsilon, \tag{4}$$

where the ocean eddy diffusivity $K\frac{\partial}{\partial z}$ (vertical shear) is generally parameterized as a function of the TC wind speed *wnd*, as the vertical shear becomes strong when the surface wind stress is strong. The vertical temperature gradient $\frac{\partial T}{\partial z}$ is simply represented by $\frac{1}{SSH}$, as low SSH in general indicates a shallow thermocline and sharp temperature gradient (i.e, over the continental shelf), and verse visa. Moreover, warm and cold eddies having a diameter of several hundred kilometers with raised and depressed SSH anomalies of ±20 cm are very common in the ocean (Lin et al., 2008), which can be represented by the SSH as well. The Ekman-induced upwelling depends largely on the TC cyclonic wind curl $curl\left(\frac{\tau}{\rho f}\right)$, as the greater the TC cyclonic vorticity, the greater the upwelling. The upwelling is proportional inversely to the TC translation speed *SPD*, as low-moving TC exerts wind stress over the ocean surface for a longer time. Thus, the advection term (ADV) is simply represented by $\frac{curl(\tau)}{SPD}$. The surface heat flux term is represented by $\frac{Q}{SSH}$, where the SSH is used as an indicator for the depth of ocean mixed layer.

The weighting coefficients *a*, *b*, *c* and *d* can be determined for each selected typhoon using a least-squares fit. Figure 6 shows the fitting results for the 100 TCs indexed by their case number. Coefficients *a*, *b* and *c* all fall into a narrow range implying a generally stable fitting. *a* are all positive, indicating that the winds always make the SST cooling, given that $\frac{wnd}{SSH}$ is always positive. Likewise, positive *b* (upwelling) indicates a SST cooling and negative *b* (downwelling) indicates a SST warming. Positive *c* (ocean gains heat) indicates a SST warming and negative *c* (ocean losses heat) indicates a SST cooling. ε indicates misfits, showing an average fitting error of 0.07, given the normalized variables. The fitness also can be measured by the correlation coefficient (*r*) and the mean absolute errors (MAE) between the observed and diagnostic SST (Figs 6e to f). We see that the correlation coefficients range from 0.2 to 0.7 with a mean value of about 0.5 and the MAE is averaged on 0.72°C. Given an average SST cooling of 3.4°C for all 100 TCs, this error indicates an overall good fitting.

Different from most previous studies based on numerical simulations, we obtained the TC-SSTC from an observational point of view. As shown, the regression model is able to separate reasonably well the three dynamic and thermodynamic processes, although it still includes uncertainties. Figure 7 shows the relative contributions (percentages) of the three processes to the total SST cooling. The wind-induced vertical mixing is apparently the most dominant factor, with a much higher percentage (55.2%) than that of the advection term (18.4%) and heat flux term (26.3%). This result is in a very good agreement with previ-

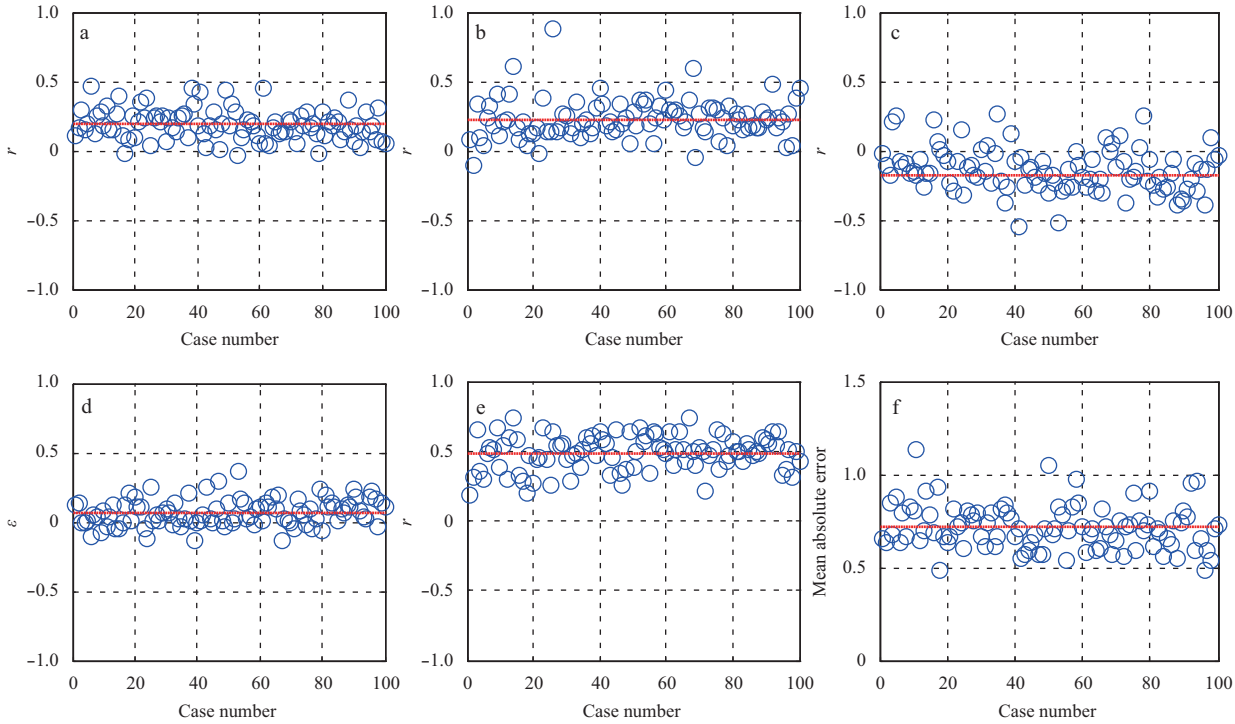

Fig. 6. Fitted parameters of the diagnostic model in Eq. (4). a. Coefficient of mixing term, b. coefficient of advection term, c. coefficient of heat flux term, d. ε, e. correlation coefficient between ΔSST_{diag} and ΔSST_{obs}, and f. mean absolute error between theobserved and diagnostic SST (MAE, °C). Red lines indicate the mean values.

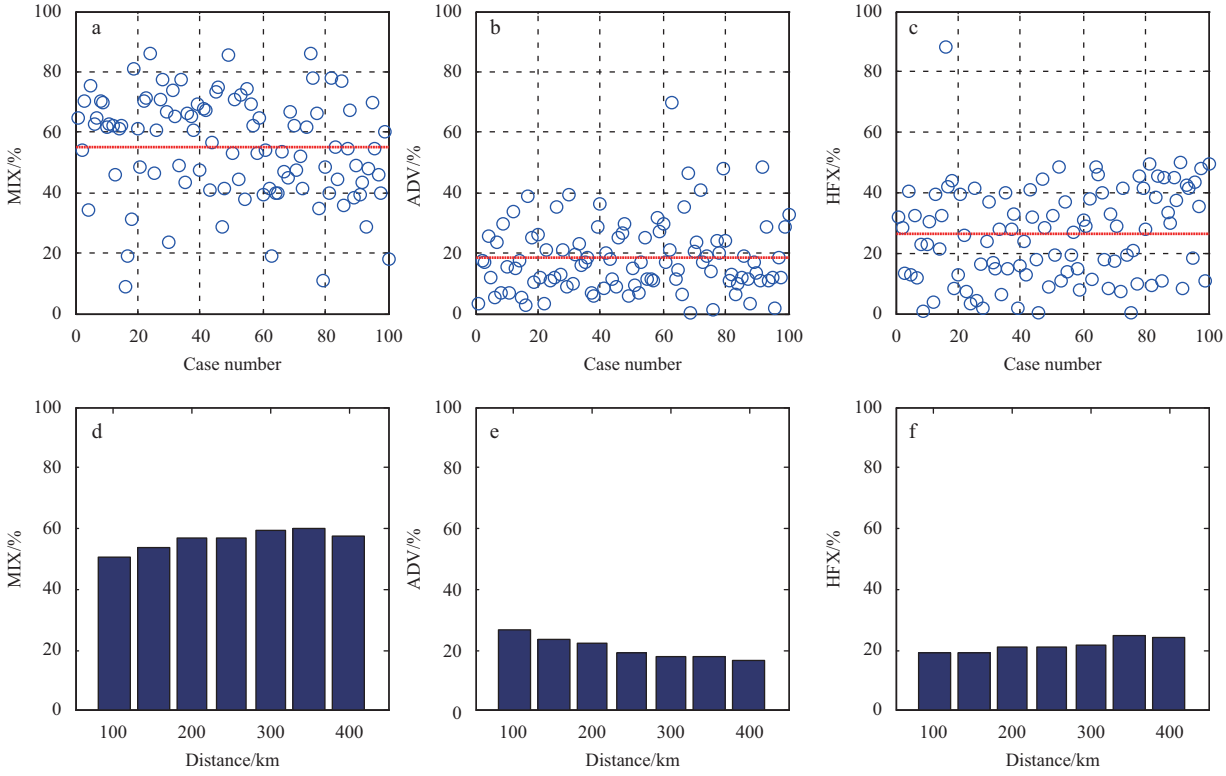

Fig. 7. Contributions of temperature budget terms to the total SST cooling: a. Mixing, b. advection and c. heat flux; and distributions of temperature budget terms verse distance to TC centers: d. mixing, e. advection and f. heat flux. Red lines indicate their mean.

ous model studies (Price, 1981; Jacob et al., 2000; Wei et al., 2014). We noticed that the contribution of the vertical mixing could be less than 20% for some TC cases (Fig. 7a), indicating that the wind effect does not always dominate under certain conditions. Accordingly, the contributions of the advection and heat flux terms can be more than 40% of the total SST cooling (Figs 7b

and c). On the other hand, the relative contributions of the three terms can be averaged along radial distances to the TC centers (Figs 7d to f). The fitting percentages were averaged on a bin of 50 km interval. It is shown that the contributions of the vertical mixing and heat flux terms increase with distance, while the upwelling is significant near the TC center and decreases away from the TC center. The strong upwelling near the TC center is mainly associated with the Ekman pumping, parameterized by the wind curl.

3.3 *Sensitivity tests on parameterizations*

In the regression model, a total of five variables were chosen for the right hand side terms of Eq. (4), implying that there are many combinations of using different variables. To examine the sensitivity of the model performance to the selections of the variables, we carried out a set of sensitivity tests with different configurations shown in Table 1. The CTL denotes the control results described above. For sensitivity tests on TC winds, we carried out the regression of Eq. (4) using those TCs with their maximum wind speeds exceeding 25, 35 and 45 m/s, respectively. Similarly, a set of sensitivity tests were carried out for the TC moving speed, the SST cooling, the SSH and the ocean depth. First of all, the overall small ε and MAEs for all tests confirm that the regression model is very stable. Furthermore, the averaged contributions of the vertical mixing increase with TC intensity, accounting for up to 71.2% of the total SSTC for those TCs with wind speeds being greater than 45 m/s, and both advection and heat flux effects decrease for compensation. In contrast, the vertical mixing effect is relatively less important in tropical regions (48.2%) and over the continental shelf (44.8% for depth being less than 200 m), where the heat flux effects increase to 36.2% and 37.7%, respectively. This can be attributed partly to the shallow depth with homogenous high temperature throughout the water column (Price, 2009), and partly to deep thermocline in tropics. Contributions of the advection effect are relatively stable, sensitive mainly to the TC translation speed. It is noteworthy that for those TCs producing very strong SST cooling (>4°C), contributions of the three budget terms are almost equally important (40.8%, 24.9% and 34.4%, respectively). This is usually happened to those strong and slow-moving TCs over the continental shelf. These sensitivity results confirm that the wind effect is overall the predominant factor, but can be modulated by the advection and heat flux effects under different atmospheric and oceanic conditions.

The regression model is based on a linear assumption, however in reality the three processes are nonlinearly interacted with each other. To understand the roles of each process, most of previous studies attempted to separate the dynamic processes (vertical mixing and upwelling) and thermodynamic process (heat flux forcing). Price (1981) isolated the upwelling effect by switching off nonlinear terms in their model. Uhlhorn and Shay (2013) applied a linear temperature budget analysis on simulations of a fully nonlinear model. Wei et al. (2014) considered the vertical mixing and heat flux terms as one term (entrainment) to separate it from upwelling. In this study, we realize that the resolution (2.5°×2.5°) of the original NCEP heat flux forcing is much coarser than other variables. In order to compare with the previous results, we have carried out the regression fitting by removing the heat flux term $\frac{Q}{SSH}$, so that the heat flux effect will be integrated into the vertical mixing and upwelling effects. Figure 8 show the contributions of the vertical mixing and the upwelling terms. The averaged contributions of the vertical mixing and advection terms increase to 77% and 23% respectively, agreeing well with 75% and 25% in Wei et al. (2014) and 85% and 15% in Price (1981). It is noted that the upwelling contributions can be more than 90% for a few TC cases, in which the vertical mixing effect is insignificant instead.

4 Summary and discussion

Combining the linear regression and the temperature budget formula, a regression model was proposed to parameterize the TC-induced SST cooling. The three major processes underlying the SST cooling (vertical mixing, upwelling and heat flux forcing) were parameterized empirically using five atmospheric and oceanic variables: SSH, wind speed, wind curl, TC translation speed and surface heat flux. The regression model fits well to the 10-year statistical observations/reanalysis data from 100 selected TCs in the northwestern Pacific during 2001–2010, with an averaged fitting error of 0.07 and a mean absolute error of 0.72°C. According to the fitting results, the vertical mixing is the predominant process producing the SSTC, accounting for 55% of the total cooling. The upwelling accounts for 18% of the total cooling and its maximum occurs near the TC center, associated with TC-induced Ekman pumping. Surface heat flux accounts for 26% of the total cooling and increases towards the tropics and the continental shelf. Sensitivity tests on the model parameterizations indicate that the wind effect is overall the most dominant factor to the SST cooling, but can be significantly modulated by the upwelling and heat flux effects under certain atmospheric and oceanic conditions.

The dominant role of the wind-induced vertical mixing and the associated entrainment process has been well interpreted in most previous studies focusing on individual TC cases and using numerical simulations, while in this study the contribution of the vertical mixing ranges from 10% to 90% from the statistical fitting with 100 TCs (Fig. 7a). This implies that the dominant role of the vertical mixing could be significantly modulated by the upwelling and heat flux forcing. On the other hand, the upwelling and heat flux effects vary in different studies. The earliest work can be traced back to Price (1981), who finds that the upwelling and heat flux effect are negligible (≈3%) for slow-moving TC and are significantly important (≈28%) for fast-moving TC. Jacob et al. (2000) and Tsai et al. (2008) found that the upwelling effect varied from 10% to 80% with different numerical schemes. Wei et al.

Table 1. Sensitivity tests on the regression model

	TC wind/m·s^{-1}				TC speed/m·s^{-1}			ΔSST/°C				SSH/cm			Depth/m		
	CTL	25–35	35–45	>45	CTL	>4	<4	CTL	2–3	3–4	>4	CTL	<150 cm	>150 cm	CTL	<200 m	>200 m
ε	0.07	0.07	0.07	0.06	0.07	0.10	0.11	0.07	0.03	0.03	0.07	0.07	0.23	0.08	0.07	0.12	0.06
r	0.50	0.50	0.54	0.58	0.50	0.46	0.47	0.50	0.40	0.34	0.33	0.50	0.46	0.49	0.50	0.46	0.49
MAE/°C	0.72	0.72	0.77	0.82	0.72	0.69	0.70	0.72	0.62	0.57	0.53	0.72	0.62	0.73	0.72	0.67	0.71
MIX/%	55.2	56.2	58.4	71.2	55.2	54.6	48.5	55.2	47.6	43.9	40.8	55.2	48.2	51.8	55.2	44.8	57.4
ADV/%	18.4	17.7	15.6	14.3	18.4	13.6	22.6	18.4	21.9	23.2	24.9	18.4	15.6	20.1	18.4	17.4	18.1
HFX/%	26.3	26.1	26.0	14.5	26.3	31.8	28.8	26.3	30.5	32.9	34.4	26.3	36.2	28.1	26.3	37.7	24.5

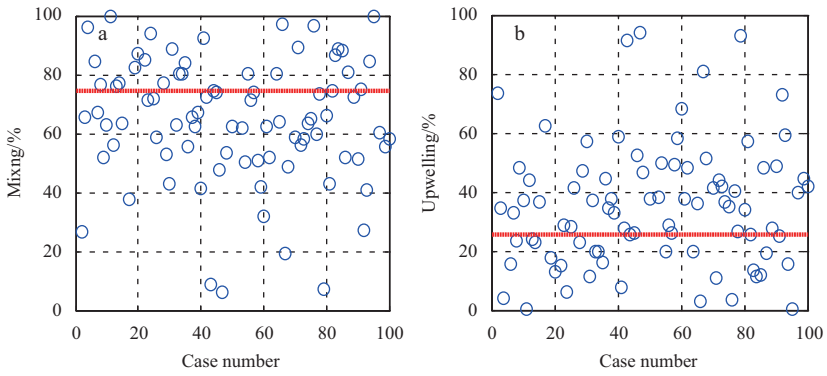

Fig. 8. Contributions of temperature budget terms to the total SST cooling. a. Vertical mixing, and b. advection-induced upwelling. Red lines indicate their mean.

(2014) find that the upwelling can be neglected when a TC is approaching, but can be up to 71% after a TC's passage. In this study, the upwelling effect ranges from 1% to 70% and the heat flux effect from 1% to 50% (Figs 7b and c), indicating more diverse TC conditions and ocean responses. Furthermore, the sensitivity results indicate that the upwelling effect is more sensitive to TC intensities and translation speeds than to ocean conditions (SSH and depth), which is also consistent with Price (1981). The heat flux effect is sensitive to both atmospheric and oceanic conditions.

The SSTC is a complex process, involving multiple temporal and spatial scales, for example, the vertical mixing associated with mesoscale sustained winds throughout the TC's life cycle, the upwelling associated with ocean divergent flows persisting for a much longer time after the TC's passage, and the TC-induced near-inertial waves with an inertial period of approximately 1.2 d. However, due to relatively coarse resolutions (daily) of the reanalysis data used and the linear assumption, the regression model cannot reproduce all these multiscale transient processes. For instance, the near-inertial waves obviously were filtered out, while the vertical mixing, upwelling and heat flux effects with larger scales were included. On the other hand, the SSTC also involves instantaneous feedbacks between the TCs and the ocean. However, the data used in the regression model consist primarily of satellite data derived from different projects with different qualities. In particular, it is well known that the CCMP winds are usually underestimated compared with observations (Jacob and Shay, 2003; Wang et al., 2012). TMI SST maps were derived from a three-day running mean of original images. Therefore, due to these deficiencies, the regression model is unable to reproduce a transit state of the SSTC.

Although the physical mechanisms driving the SSTC in response to typhoons have been interpreted in many previous studies, to our best knowledge, the SSTC effect has not been included in any weather forecast models, which may lead to a systematic warm bias for modeling storm intensities. To account for the SSTC effect, time-dependent satellite SSTs are often used as the ocean surface conditions (Chelton, 2005; Zhu and Zhang, 2006; Vincent et al., 2012). However, the daily-averaged SST cannot provide enough cooling to inhibit intensification of storms. Given the typhoon-induced ocean inertial response $\frac{\partial u}{\partial t} = fv$, taking $u/v \approx 10^{-1}$ m/s and $f \approx 10^{-4}$ s^{-1}, the response time is approximately 10^4 s, much shorter than the time resolution of the satellite SSTs (1 d). Therefore, daily-averaged SSTs may result in a significant displacement of the cooling relative to the typhoon center, which may lead to a spatial bias for modeling typhoon structure and intensity. In contrast, the SSTC parameterization scheme carries out its calculation at every model time step, much shorter than the ocean response time (10^4 s), and therefore can provide an instantaneous SSTC feedback to typhoon development.

Acknowledgements

The authors thank NCEP-DOE for providing surface heat flux data (http://www.esrl.noaa.gov/), the UCAR for providing CCMP wind product (http://rda.ucar.edu/datasets/ds744.9/), the JTWC for providing TC information (http://www.usno.navy.mil/JTWC), the AVISO for providing ocean SSH data (http://www.aviso.oceanobs.com) and the NASA/TRMM/TMI program for providing daily SST maps (http://pmm.nasa.gov/TRMM).

References

Bender M A, Ginis I. 2000. Real-case simulations of hurricane-ocean interaction using a high-resolution coupled model: effects on hurricane intensity. Mon Wea Rev, 128(4): 917–946

Braun S A. 2002. A cloud-resolving simulation of Hurricane Bob (1991): storm structure and eyewall buoyancy. Mon Wea Rev, 130(6): 1573–1592

Chelton D B. 2005. The impact of SST specification on ECMWF surface wind stress fields in the eastern tropical Pacific. J Climate, 18(4): 530–550

Chen Hua, Zhang Dalin, Carton J, et al. 2011. On the rapid intensification of Hurricane Wilma (2005): Part I. Model prediction and structural changes. Wea Forecasting, 26(6): 885–901

Cione J J, Uhlhorn E W. 2003. Sea surface temperature variability in hurricanes: implications with respect to intensity change. Mon Wea Rev, 131(8): 1783–1796

Ginis I. 2002. Tropical cyclone-ocean interactions. Atmosphere-Ocean Interactions, Advances in Fluid Mechanics Series, No. 33. Boston: WIT Press, 83–144)

Huang Peisheng, Sanford T B, Imberger J. 2009. Heat and turbulent kinetic energy budgets for surface layer cooling induced by the passage of Hurricane Frances (2004). J Geophys Res, 114(C12): C12023, doi: 10.1029/2009JC005603

Jacob, S. D., Shay, L. K. 2003. The role of oceanic mesoscale features on the tropical cyclone–induced mixed layer response: A case study. Journal of physical oceanography, 33(4), 649–676.

Jacob S D, Shay L K, Mariano A J, et al. 2000. The 3D oceanic mixed layer response to Hurricane Gilbert. J Phys Oceanogr, 30(6): 1407–1429

Jaimes B, Shay L K. 2009. Mixed layer cooling in mesoscale oceanic eddies during Hurricanes Katrina and Rita. Mon Wea Rev, 137(12): 4188–4207

Jullien S, Menkes C E, Marchesiello P, et al. 2012. Impact of tropical cyclones on the heat budget of the south pacific ocean. J Phys Oceanogr, 42(11): 1882–1906, doi: 10.1175/jpo-d-11–0133.1

Lin I I, Wu C C, Emanuel K A, et al. 2005. The interaction of supertyphoon Maemi (2003) with a warm ocean eddy. Mon Wea Rev, 133(9): 2635–2649, doi: 10.1175/MWR3005.1

Lin I I, Wu C C, Pun I F, et al. 2008. Upper-ocean thermal structure and the western north Pacific category 5 typhoons: Part I. Ocean features and the category 5 typhoons' intensification. Mon Wea Rev, 136(9): 3288–3306, doi: 10.1175/2008MWR 2277.1

Lin Yanluan, Zhao Ming, Zhang Minghua. 2015. Tropical cyclone rainfall area controlled by relative sea surface temperature. Nat Commun, 6: 6591, doi: 10.1038/ncomms7591

Liu Xin, Wei Jun. 2015. Understanding surface and subsurface temperature changes induced by tropical cyclones in the Kuroshio. Ocean Dyn, 65(7): 1017–1027

Price J F. 1981. Upper ocean response to a hurricane. J Phys Oceanogr, 11(2): 153–175

Price J F. 2009. Metrics of hurricane-ocean interaction: vertically-integrated or vertically-averaged ocean temperature?. Ocean Sci, 5(3): 351–368

Price J F, Sanford T B, Forristall G Z. 1994. Forced stage response to a moving hurricane. J Phys Oceanogr, 24(2): 233–260

Sakaida F, Kawamura H, Toba Y. 1998. Sea surface cooling caused by typhoons in the Tohoku area in August 1989. J Geophys Res, 103(C1): 1053–1065

Shay L K, Black P G, Mariano A J, et al. 1992. Upper ocean response to Hurricane Gilbert. J Geophys Res, 97(C12): 20227–20248

Shay L K, Goni G J, Black P G. 2000. Effects of a warm oceanic feature on Hurricane Opal. Mon Wea Rev, 128(5): 1366–1383

Sun Jingru, Oey L Y, Chang R, et al. 2015. Ocean response to Typhoon Nuri (2008) in western Pacific and South China Sea. Ocean Dyn, 65(5): 735–749, doi: 10.1007/s10236–015-0823–0

Tsai Y, Chern C S, Wang J. 2008. Typhoon induced upper ocean cooling off northeastern Taiwan. Geophys Res Lett, 35(14): L14605

Uhlhorn E W, Shay L K. 2013. Loop current mixed layer energy response to Hurricane Lili (2002): Part II. idealized numerical simulations. J Phys Oceanogr, 43(6): 1173–1192

Vincent E M, Lengaigne M, Madec G, et al. 2012. Processes setting the characteristics of sea surface cooling induced by tropical cyclones. J Geophys Res, 117(C2): C02020, doi: 10.1029/2011 JC007396

Wei Jun, Liu Xin, Wang Dongxiao. 2014. Dynamic and thermal responses of the Kuroshio to typhoon Megi (2004). Geophys Res Lett, 41(23): 8495–8502, doi: 10.1002/2014GL061706

Wu C R, Chang Y L, Oey L Y, et al. 2008. Air-sea interaction between tropical cyclone Nari and Kuroshio. Geophys Res Lett, 35(12): doi: 10.1029/2008GL033942

Zhu Tong, Zhang Dalin. 2006. The impact of the storm-induced SST cooling on hurricane intensity. Adv Atmos Sci, 23(1): 14–22